

## Polyvinyl pyrrolidone as a Corrosion Inhibitor for Carbon Steel in HCl

Layla A. Al Juhaiman

Chemistry Department, Faculty of Science, King Saud University, Riyadh, Saudi Arabia  
E-mail: [ljuhiman@ksu.edu.sa](mailto:ljuhiman@ksu.edu.sa)

Received: 14 December 2015 / Accepted: 19 January 2016 / Published: 1 February 2016

---

The inhibition effect of the green inhibitor Polyvinyl pyrrolidone (PVP) on the corrosion of carbon steel (C-steel) in 2 M HCl aerated unstirred solutions is investigated. Electrochemical methods (EIS and potentiodynamic polarization) and gravimetric methods are applied to study the corrosion of C-steel with PVP over a range of concentrations and temperatures. The polarization method indicates that PVP behaves as a mixed-type inhibitor. The impedance method reveals that the charge transfer process is dominant in controlling the corrosion of C-steel. The inhibition efficiencies ranged from 56–83%, as determined by weight loss, and from 60–90%, as determined by electrochemical methods. The different techniques used confirm the adsorption of PVP on the C-steel surface and consequently the inhibition of the corrosion process. The adsorption of PVP on the C-steel surface is found to obey the Langmuir adsorption isotherm. A mechanism is proposed to explain the inhibitory action of PVP. The thermodynamic parameters for the adsorption of PVP on the C-steel surface show a decrease in  $E_{app}$ ,  $\Delta H$  and  $\Delta S$ . The inhibition efficiency of PVP increases with increasing inhibitor concentration and increasing temperature.

---

**Keywords:** C-steel; HCl; PVP inhibitor; EIS and potentiodynamic polarization; gravimetric methods; Thermodynamic parameters; Adsorption mechanism.

### 1. INTRODUCTION

Iron and its alloys are extensively used in industry especially for structural applications. However, their susceptibility to rusting in a humid atmosphere and their high dissolution rate in acidic media are the major obstacles to facilitate their use on a large scale. Acidizing of petroleum in oil wells is an important technique for enhancing oil production. This process involves using a solution of 15–28% hydrochloric acid. However, inhibitors are added to the acidic solution during the acidizing process to reduce the aggressive corrosive effects of the acid on tubing and casing materials. Inhibitors are widely used for the protection of metals to corrosion in acidic environments. Inhibitors usually

protect the metal by adsorbing on the surface and retarding metal corrosion in aggressive media. Therefore, selecting the appropriate inhibitor for a particular metal is very important. Most of the well-known inhibitors are organic compounds containing nitrogen [1], oxygen [2, 3] or food extract [4]. Some studies have shown that the inhibition of the corrosion process is made mainly by the formation of donor–acceptor surface complexes between the free- or  $\pi$ -electrons of an inhibitor and the vacant d orbital of the metal [5, 6]. The environmentally friendly inhibitors, or green inhibitors, have recently been receiving more attention. Among these are Polyvinyl pyrrolidone [4], poly ethylenimine [1] and caffeic acid [2]. A considerable number of studies have been published on the inhibition of steel and its alloys in acidic medium [7–16].

Polyvinyl pyrrolidone was found to be a good corrosion inhibitor in alkaline solutions containing NaCl [4] and in neutral solutions [17]. The aim of the present study is to investigate the inhibition of carbon steel (C-steel) corrosion by Polyvinyl pyrrolidone (PVP) in aerated, unstirred 2 M HCl solutions. Electrochemical methods (EIS and Potentiodynamic polarization) and gravimetric (weight loss) methods are applied. The thermodynamic parameters were evaluated and a mechanism is proposed to explain the inhibitory action of this green corrosion inhibitor.

## 2. MATERIALS AND METHODS

### 2.1. Materials

C-steel was obtained from ODS company (Germany). Circular discs (d=2.97 cm, thickness=0.6 cm) were used with the following composition by percentage weight: C=0.46, Mn=0.60, Si=0.17, P=0.016, S=0.008, Cr=0.17, Ni=0.05, Mo=0.01, Cu=0.06, Al=0.025 and the remainder is Fe. Polyvinyl pyrrolidone (PVP) was purchased from Sigma Aldrich. The molecular weight of PVP is 8000 g/mol. The chemical structure of PVP is shown in Figure 1. The blank solution was 2M HCl prepared from dilution of concentrated HCl solution (from BDH). The concentration of the solution was ascertained by standardizing with sodium bicarbonate. The test solutions were prepared by dissolving a certain weight of PVP solid in a volumetric flask with the required volume of the concentrated HCl to make the final concentration of PVP range between 800-2000 ppm.

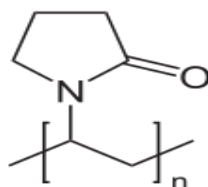


**Figure 1.** Structure of PVP.

### 2.2. Experimental Methods

#### 2.2.1. Electrochemical Measurements

The electrochemical measurements were performed using a potentiostat/galvanostat (ACM) connected to a computer. A three electrode cell assembly, consisting of a C-steel rod embedded in

araldite as the working electrode (WE), a platinum sheet as the counter electrode (CE) and a saturated calomel electrode as the reference electrode (RE), was used for the electrochemical measurements. The temperature of the electrolyte was maintained at the required temperature using a water bath. Before immersion in the test solutions, the WE was polished with a polishing machine (Metaserve) using emery paper from 600 to 1200 grade until a mirror image was obtained. Then, the WE was washed with distilled water then immersed in acetone for 1 minute in an ultrasonic cleaner (Cole Palmer). The WE electrode was prepared directly before electrochemical measurements then immersed in the test solution at open circuit potential for one hour until a steady state potential was obtained before impedance and polarization measurements were performed. All experiments were performed in aerated solutions. From the polarization data, the degree of surface coverage ( $\theta$ ) and the percentage inhibition efficiency (% IE) were calculated.

EIS was carried out using AC signals (10 mV) peak-to-peak at an open circuit potential in the frequency range of 30 kHz–0.05 Hz. Impedance data in this work were represented by Nyquist plots.

After EIS measurements, polarization measurements were applied. The potential was scanned with a scan rate of 25 mV/min from the cathodic to anodic direction so that the maximum over voltage was  $\pm 250$  mV from  $E_{ss}$ . Corrosion current densities ( $I_{corr}$ ) and Tafel slopes were calculated. All of the experiments were performed in triplicate to ensure reproducibility.

### 2.2.2. Weight-loss Measurements

The C-steel discs (area  $\approx 19.65$  cm<sup>2</sup>) were polished with a polishing machine (Metaserve) using emery paper (600–1200 grade) until a mirror image was obtained. The discs were washed with distilled water and cleaned with acetone in an ultrasonic cleaner (from Cole Palmer). Before immersion in the test solutions, the dimensions of each disc were ascertained. For weight loss (WL) experiments, the cleaned C-steel discs were weighed ( $\pm 0.0001$  g, Mettler Toledo) before immersion in 50 ml of the test solution for one hour at the required temperature using a thermostated water bath. At the end of the run, the discs were washed with distilled water then acetone in an ultrasonic cleaner, dried and immediately weighed. The weight loss was determined. The average weight loss for each two identical experiments was taken and expressed in mg.

## 3. RESULTS AND DISCUSSION

### 3.1. Electrochemical Measurements

#### 3.1.1 EIS Measurements

The Nyquist plots for HCl in the presence and absence of different inhibitor concentrations, ranging from 2000–8000 ppm, are presented in Figure 2. The shapes of the impedance plots for the inhibited electrodes are not substantially different from those of the uninhibited electrodes (not shown). The presence of the inhibitor increases the Nyquist plots semicircle but does not change other

aspects of the behavior. It is shown that the impedance response consisted of the characteristic semicircles, indicating that the dissolution of the C-steel process occurs under charge transfer control; hence, under activation control [18]. The charge transfer resistance values ( $R_{ct}$ ) were obtained from the diameter of the semicircles of the Nyquist plots. The value of  $R_{ct}$  is a measure of the electron transfer across the C-steel surface and is inversely proportional to the corrosion rate. These semicircles are of capacitive type whose diameters increase with increasing the inhibitor concentrations and indicate an increase of the inhibition properties [19–25]. Similar Nyquist plots were obtained from previous studies for inhibitors containing nitrogen, such as pyrazolone [8], aliphatic amines [21], and poly(aniline-formaldehyde) [22].

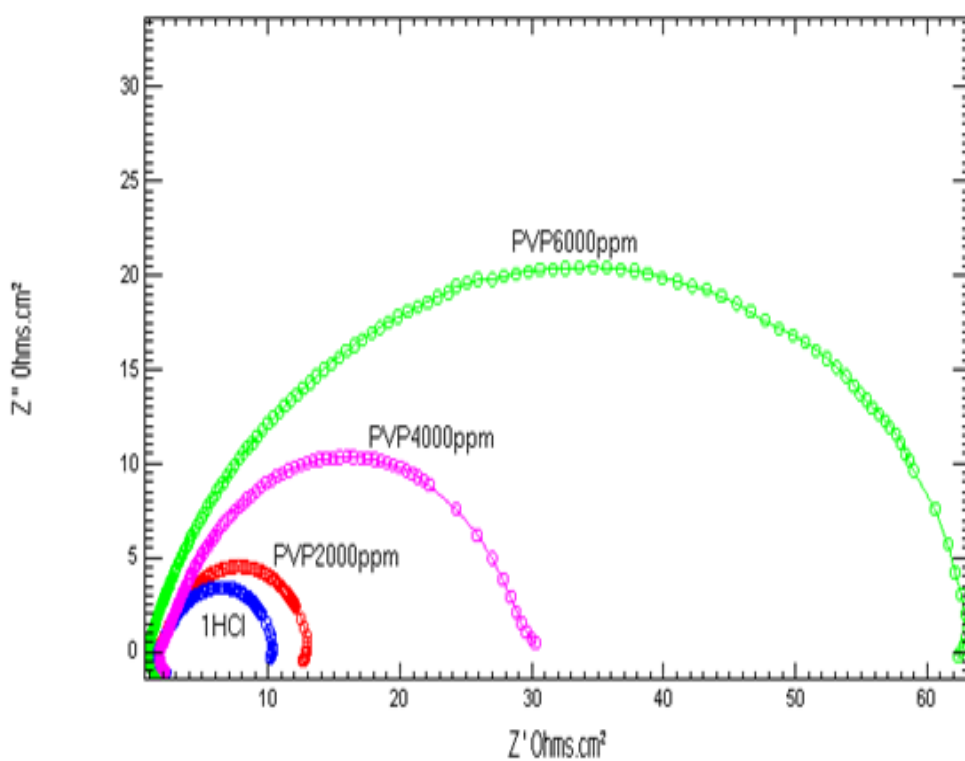


**Figure 2.** EIS plots for HCl in the presence and absence of different inhibitor concentrations.

The EIS plots show a depressed capacitive loop in the high frequency range and an inductive loop in the low frequency range. The capacitive loop usually arises from the time constant of the electric double layer and charge transfer resistance [18]. The inductive loop originates from the adsorption relaxation of intermediates, which may cover the reaction surface. The depressed form of the higher frequency loop reflects the surface inhomogeneity of interfacial or structural origin, as those found in adsorption processes [18]. Thus, in the present study, the system could be described by a simple equivalent circuit model, which is the well-known Randle cell, as shown in Figure 3. In this equivalent circuit,  $R_s$  is the solution resistance,  $R_{ct}$  is the charge transfer resistance,  $C_{dl}$  represents the capacitance elements. The capacitor, in the equivalent circuit is a frequency dependent element related to the surface roughness [18].

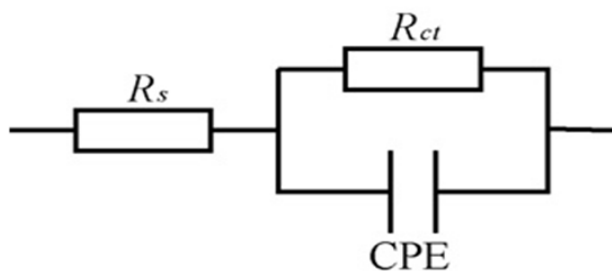


**Figure 3.** The equivalent circuit model used to fit the experimental EIS data.

The double layer capacitance,  $C_{dl}$  was obtained at the frequency  $f_{max}$  (where the imaginary component of the impedance is a maximum) by the following equation:

$$C_{dl} = \frac{1}{2\pi R_{ct} f_{max}} \tag{1}$$

The inhibition efficiency (% IE) and surface coverage ( $\theta$ ) are calculated from the following equations:

$$\theta = \left(1 - \frac{R_{ct}^0}{R_{ct}}\right) \tag{2}$$

$$\% \text{ IE} = \theta \times 100 \tag{3}$$

Where  $R_{ct}^0$  is the impedance of the inhibitor free solutions and  $R_{ct}$  is the impedance of the acid + PVP solutions.

The values of  $R_{ct}$ ,  $C_{dl}$ ,  $\theta$  and % IE for C-steel in 2 M hydrochloric acid containing different concentrations for PVP inhibitor are shown in Table 1. The present data reveals that the  $R_{ct}$  values increase with increasing inhibitor concentration while the  $C_{dl}$  values decrease. The %IE and surface coverage values increase with increasing inhibitor concentration. The present EIS plots are similar to those reported by Ashaai-Sorkhabi for certain polyethylene glycols in HCl [19].

**Table 1.** EIS data for C-steel in 2 M HCl in the absence and presence of different concentrations of PVP.

Solution	$R_{sol}$ ( $\Omega \cdot \text{cm}^2$ )	$R_{ct}$ ( $\Omega \cdot \text{cm}^2$ )	$C_{dl}$ ( $\mu\text{F}$ )	$\theta$	% IE
2M HCl	1.577	11.60	5306	---	---
2000ppm PVP	0.881	63.9	1117	0.789	81.8
4000ppm PVP	1.63	77.56	1114	0.790	85.0
6000ppm PVP	1.4	80.78	1018	0.808	85.6
8000ppm PVP	1.5	88.78	753	0.858	86.9

The increase in  $R_{ct}$  values may be attributed to the adsorption of the inhibitor molecules at the metal surface and the formation of a protective film on the metal/solution interface, as reported by others [7, 13, 16]. The decrease in  $C_{dl}$  values results from a decrease in the local dielectric constant and/or an increase in the thickness of the double layer, suggesting that the inhibitor molecules inhibit

the iron corrosion by adsorption at the metal/acid interface [7, 16]. Furthermore, the decrease in  $C_{dl}$  values could be attributed to the adsorption of PVP molecules at the metal surface [20] and the replacement of water molecules at the electrode interface by the organic inhibitor of lower dielectric constant through adsorption [21].

### 3.1.2 Polarization Measurements (Tafel method)

Typical potentiodynamic polarization curves for the C-steel in 2 M HCl in the presence and absence of different concentrations of PVP are shown in Figure 4. The respective Tafel parameters, inhibition efficiency (% IE) and surface coverage ( $\theta$ ) are provided in Table 2. It is clear that the shapes of the Tafel plots for the inhibited electrodes are not substantially different from those of the uninhibited electrodes. The presence of the inhibitor decreases the current density but does not change other aspects of the behavior. It is evident from Table 2 that the adsorption of the inhibitor shifted the corrosion potential ( $E_{corr}$ ) in the positive direction. The addition of PVP decreases both of the Tafel slopes ( $\beta_a$  and  $\beta_c$ ), the anodic and cathodic Tafel slopes. This indicates that PVP is a mixed-type inhibitor affecting the iron dissolution and hydrogen evolution [15, 16]. The reduction of the positive and negative currents in the presence of PVP can be explained by the blocking of active sites by the formation of a protective film on the surface of the electrode [22, 23]. The values of the surface coverage and inhibition efficiency reached its maximum at a PVP concentration of 6000 and remained almost constant from 4000–8000 ppm.

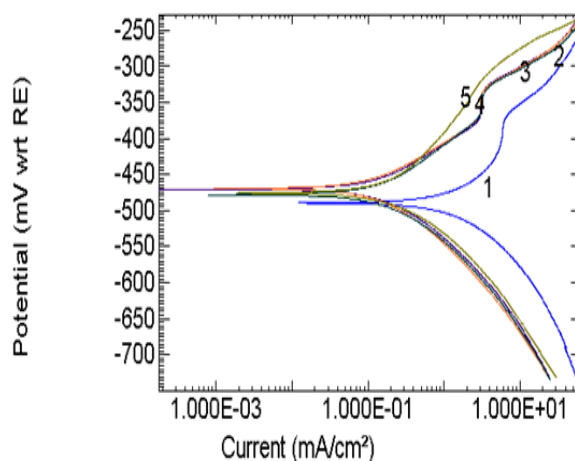


**Figure 4.** Tafel plots for C-steel at 30 °C (1=2 M HCl, 2=8000 ppm PVP, 3=6000 ppm PVP, 4= 4000 ppm PVP, 5=2000 ppm PVP).

As can be seen from Table 2, the PVP inhibitor reduced both the anodic and cathodic currents with a slight shift in the corrosion potential (22 mV). If the displacement in the corrosion potential is more than 85 mV, with respect to the corrosion potential of the blank solution, the inhibitor can be designated as a cathodic or anodic type [23]. In the present study, the displacement was approximately 22 mV, which indicated that the studied inhibitor is a mixed-type inhibitor which is in agreement with

some other studies [16]. These results support the results from the EIS measurements, which showed that the inhibitor does not alter the electrochemical reactions responsible for corrosion. Rather, the inhibition of metal corrosion arises primarily from its adsorption on the metal surface, as found by previous studies [15, 16, 19, 22, 24, 25].

**Table 2.** Tafel parameters for C-steel at 30 °C in 2 M HCl in the absence and presence of different concentrations of PVP.

Solution	$-E_{\text{corr}}$ (mV)	$i_{\text{corr}}$ (mA/cm <sup>2</sup> )	$\beta_a$ (mV/dec)	$-\beta_c$ (mV/dec)	EI	$\theta$
2M HCl	500	0.670	79	70	--	--
2000ppm PVP	478	0.170	78	56	74.6	0.746
4000ppm PVP	476	0.106	55	56	84.2	0.842
6000ppm PVP	474	0.068	59	54	89.9	0.899
8000ppm PVP	477	0.070	58	55	89.5	0.895

### 3.2. Gravimetric Method (Weight Loss)

Weight loss is a non-electrochemical technique for the determination of corrosion rates and inhibitor efficiency. This method provides more realistic results than the electrochemical techniques because the experimental conditions are approached in a manner which resembles the real-life conditions. However, immersion tests are time-consuming. The weight loss of C-steel discs was evaluated over one hour of immersion in 2 M HCl solutions in the absence and presence of different concentrations of PVP.

#### 3.2.1. Effect of Inhibitor Concentration

Corrosion rate (CR) from WL was calculated using the following equation:

$$\mathbf{CR} = \frac{\Delta \mathbf{W}}{\mathbf{A} * \mathbf{t}} \quad (4)$$

Where  $\Delta W$  is the weight loss of C-steel (mg);  $A$  is the surface area (cm<sup>2</sup>) of C-steel discs and  $t$  is the immersion time (hours). The inhibition efficiency (% IE) and surface coverage ( $\theta$ ) are calculated from the following equations:

$$\theta = \left( 1 - \frac{\mathbf{CR}}{\mathbf{CR}^0} \right) \quad (5)$$

$$\% \text{ IE} = \theta \times 100 \quad (6)$$

Where  $\text{CR}^0$  and  $\text{CR}$  are the corrosion rates in the absence and presence of PVP, respectively.

The corrosion rate was calculated for the acid in the absence and presence of different concentrations of PVP in the range of  $(2.50\text{--}10.0) \times 10^{-4}$  M. The results are shown in Table 3. The corrosion rate decreases with increasing inhibitor concentration and the inhibition efficiency increases

with increasing inhibitor concentration from 56% to 87.6%. These results indicate that PVP is a good corrosion inhibitor for C-steel in HCl medium.

**Table 3.** Corrosion rates and inhibition efficiencies at 30°C for C-steel from WL in the absence and presence of different concentrations of PVP.

Solution	CR(mg/cm <sup>2</sup> .hr)	% IE	$\theta$
2M HCl –Blank	2.50	---	---
2000ppm PVP ( $2.5 \times 10^{-4}$ M)	1.11	56.0	0.56
3000ppm PVP ( $3.75 \times 10^{-4}$ M)	1.02	60.0	0.6
4000ppm PVP ( $5.0 \times 10^{-4}$ M)	0.99	60.4	0.604
5000ppm PVP ( $6.25 \times 10^{-4}$ M)	0.84	66.4	0.664
6000ppm PVP ( $7.5 \times 10^{-4}$ M)	0.69	72.4	0.724
8000ppm PVP ( $10.0 \times 10^{-4}$ M)	0.43	87.6	0.828

It is difficult to compare the inhibition efficiency from the present study (a polymer containing a pyrrolidone ring) with that reported in other studies as the functional groups are different. Many previous studies have reported the inhibition of steel corrosion and its alloys by amines and nitrogen containing compounds [1, 4, 8, 9, 14, 19, 21, 22]. In some studies, the inhibitors were aliphatic amines (primary, secondary and tertiary), aromatic amines or contained nitrogen atoms linked to many different atoms, so that the resulting inhibition efficiency was a combination of different factors. The only study which used PVP was that performed by Jianguo et al., who showed that PVP at  $1 \times 10^{-3}$  M is a good inhibitor for C-steel in H<sub>3</sub>PO<sub>4</sub> with a maximum IE of 80% [1]. In the present study, it is noticeable that for the same concentration of  $1 \times 10^{-3}$  M PVP (8000 ppm), a comparable IE result of 82.8% in HCl solutions was obtained.

### 3.2.2 Effect of Temperature

Temperature is an important parameter when studying metal dissolution. It is known that the effect of temperature on the acid–metal reaction is highly complex. The corrosion rate in acid solutions, for example, increases exponentially with an increasing temperature because hydrogen evolution decreases [7]. Many changes may occur on the metal surface, such as adsorption, desorption, rearrangement or decomposition of the inhibitor. Zerga et al. [26] prepared pyridazine derivatives and studied their inhibitory effect on steel in HCl solutions. They found that the inhibitory effect (% IE) decreased from 92% at 303 K to 47% at 353 K [26]. Only a few inhibitors are effective at high temperature as they are at low temperature [23–24].

The effect of increasing temperature (from 30–60°C) on the corrosion rate of C-steel in 2 M HCl in the absence and presence of a constant concentration of PVP (4000 ppm) was studied using weight loss measurements. The results are shown in Table 4. It is observed that the inhibition efficiencies increase with increasing temperature. The CR increased 17 times for the free acid and 3.5

times for PVP + HCl solutions. This indicates that PVP is effective at high temperature, as has been reported by others [23–24].

**Table 4.** The effect of temperature on the corrosion rates of C-steel in the absence and presence of 4000 ppm of PVP.

T(°C)	2 M HCl, CR (mg/cm <sup>2</sup> .hr)	2M HCl+2000ppm PVP, CR(mg/cm <sup>2</sup> .hr)	% IE	θ
30	2.5	0.99	56.0	0.56
40	3.90	1.39	64.4	0.64
50	15.50	2.92	81.2	0.81
60	42.95	3.53	91.8	0.92

The values of the apparent activation energy  $E_{app}$  of the corrosion process in 2 M HCl in the presence and absence of PVP was calculated using the Arrhenius equation:

$$\ln k = \ln A - \frac{E_{app}}{RT} \tag{7}$$

Where  $k$  is the rate constant which is directly proportional to CR from weight loss,  $A$  is the Arrhenius constant,  $E_{app}$  is the apparent activation energy,  $R$  is the gas constant and  $T$  is the absolute temperature.

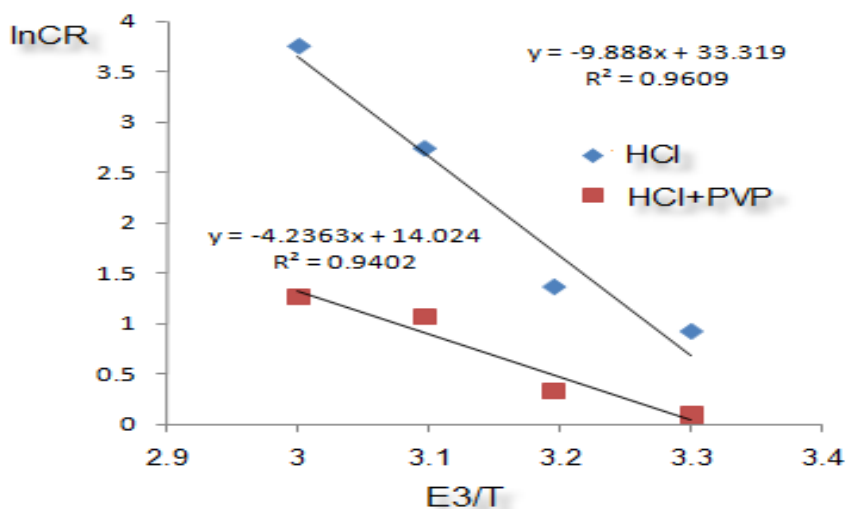


**Figure 5.** Arrhenius plots for C-steel in 2 M HCl in the presence and absence of PVP (4000 ppm).

An Arrhenius-type dependence is observed from plotting  $\ln CR$  and the inverse of  $T$  as shown in Figure 5. From the Arrhenius plots, the apparent activation energy ( $E_{app}$ ) of the corrosion process was calculated as 88.22 kJ/mol for the free acid and 35.20 kJ/mol for the acid + PVP. The  $E_{app}$  values obtained for the acid solution are close to 57.7 to 87.8 kJ/mol, that is, the range of the apparent energy

of activation commonly found for the corrosion process of mild steel in hydrochloric acid [7, 12, 24]. The  $E_{app}$  values are presented in Table 5.

Some conclusions on the mechanism of the inhibitor action can be obtained by comparing  $E_{app}$  in the presence and absence of the corrosion inhibitor. It is shown that the addition of PVP to HCl decreased  $E_{app}$ , which indicates that it is easier for PVP to be adsorbed on C-steel which agrees with previous studies [2, 9, 11, 24]. The decrease of  $E_{app}$  in the presence of PVP indicates the ease of adsorption of PVP on the C-steel surface and the decrease of the corrosion rate even at high temperatures. In addition, the decrease of  $E_{app}$  in the presence of the inhibitors is indicative of chemisorption mechanism, while higher values of  $E_{app}$  in the presence of inhibitor suggest a physical adsorption mechanism [10, 11, 24].

However, some researchers observed that the addition of the inhibitor increased the  $E_{app}$  more than  $E_{app}$  for the free acid [8, 10, 12, 25]. The increase of the activation energies in the presence of inhibitors is attributed to an appreciable decrease in the adsorption process of the inhibitor on the metal surface with increasing temperature and a corresponding increase in the corrosion rate, because of the greater area of the metal exposed to the acid [23].

To find the thermodynamic parameters, the transition state equation was applied:

$$\ln \frac{k}{T} = \left( \ln \left\{ \frac{R}{NH} \right\} + \frac{\Delta S}{R} \right) - \frac{\Delta H}{RT} \quad (8)$$

The corrosion rate from WL method was substituted for  $k$  and the values of the enthalpy were calculated from the slope, while the intercept was equal to the two terms within the brackets. The results are shown in Table 5. The values of  $\Delta H$  for the blank and the inhibitor + HCl are both endothermic, which are in agreement with other studies [9, 12]. Unlike Yurta et al. [12], who found that the value of  $\Delta H$  in the presence of the inhibitor is higher than that in its absence; Ramesh et al. [9] found that  $\Delta H$  in the presence of the inhibitor is lower than that for the blank, which agrees well with the present study and with the ease of adsorption of PVP on the C-steel surface. The positive values of  $\Delta S_{ads}$  might be explained by the following: before adsorption of inhibitor onto the steel surface, the inhibitor molecules might move freely in the bulk solution but with the progress in the adsorption process, the inhibitor molecules are disorderly adsorbed onto the steel surface, which decreases the entropy, which is in agreement with the report by Yurt et al. [12].

**Table 5.** Thermodynamic parameters from the transition state equation for the adsorption of PVP on the C-steel surface in the temperature range of 30–60 °C.

Solution	$E_{app}$ (kJ/mol)	$\Delta H$ (kJ/mol)	$\Delta S^\circ$ (kJ/Kmol)
blank	82.90	80	0.368
Inhibitor +HCl	35.24	32	0.210

The entropy of activation ( $\Delta S$ ) of the blank solution is more positive than the inhibited solution, indicating that the activated complex is represented with more randomness than the blank solution. The enthalpy of the blank solution and  $E_{app}$  are 2.5 times higher than those for the inhibitor + HCl, which indicates the ease of association of PVP on the C-steel surface.

### 3.2.3. Adsorption Mechanism

Generally, the adsorption of organic compounds occurs either directly, on the basis of donor/acceptor interactions between the p-electrons of the heterocyclic compound and the vacant d-orbitals of iron surface atoms, or by the interaction of already adsorbed chloride ions. The values of surface coverage  $\theta$  for different concentrations of PVP and at different temperatures are listed in Tables 3 and 4. The degree of surface coverage  $\theta$  at 30 °C increased with increasing concentration of PVP (from 2000–8000 ppm). Moreover, the degree of surface coverage increased with increasing temperature from 30 °C to 60 °C at 2000 ppm. This indicates that PVP works as a good inhibitor with an inhibition efficiency of 91% at 60 °C.

Careful investigation of the Tempkin, Langmuir, Frumkin and Freundlich isotherms showed that the most fitting isotherm with the maximum regression coefficients,  $R^2$  was the Langmuir isotherm.

The Langmuir adsorption isotherm may be formulated as:

$$\frac{C}{\theta} = \frac{1}{K} + C \quad (9)$$

Where  $C$  is the concentration of the inhibitor,  $\theta$  is the surface coverage and  $K$  is the equilibrium constant of the adsorption process.

A straight line relationship with a slope of almost one (0.986) was observed, as shown in Fig 6. Adherence to the Langmuir adsorption isotherm is generally regarded to indicate monolayer adsorption. The adsorption–desorption equilibrium constant  $K$  was determined from the intercept of the Langmuir isotherm while the free-energy of adsorption ( $\Delta G^\circ_{\text{ads}}$ ) was calculated according to the equation:

$$\Delta G^\circ_{\text{ads}} = -RT \ln(55.5K) \quad (10)$$

Where 55.5 is the water concentration,  $R$  is the universal gas constant, and  $T$  is the thermodynamic temperature and  $K$  is the adsorption–desorption equilibrium constant.

The adsorption–desorption equilibrium constant  $K$  was determined as 5000 L/mol, leading to  $\Delta G^\circ_{\text{ads}} = -31.57$  kJ/mol. The negative value of  $\Delta G^\circ_{\text{ads}}$  indicates that the adsorption process of the inhibitor is spontaneous, while the value of the order of more than 20 kJ/mol indicates that PVP was chemically adsorbed on the steel surface. Similar thermodynamic data were obtained for the adsorption of some triazoles [3] and 2-mercaptothiazoline on mild steel in HCl [25].

In general, the corrosion inhibition mechanism in acidic medium is the adsorption of the inhibitor onto the metal surface [1–16]. The adsorption process is influenced by the nature and the charge of the metal, by the chemical structure of the organic inhibitor, and the type of the aggressive electrolyte. The charge of the metal surface may be determined from the potential of zero charge ( $E_{\text{pzc}}$ ) [13] from the equation:

$$\Phi = E_{\text{corr}} - E_{\text{pzc}} \quad (11)$$

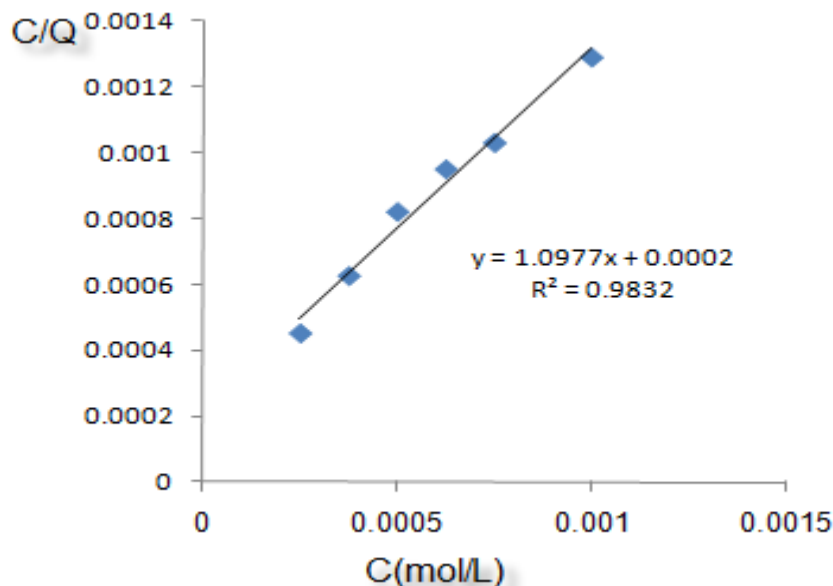


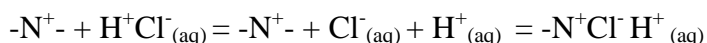
**Figure 6.** Langmuir adsorption isotherm of PVP on C-steel in 2 M HCl at 30 °C.

The potential of zero charge (pzc) is defined as the metal potential when it is measured against the reference electrode under conditions of zero charge on the metal. The ionic double layer is absent at the electrode at the potential of zero charge. At the potential of zero charge, the electrode has the greatest ability to adsorb the substance dissolved in the electrolyte solution. The ability of the electrode to adsorb organic molecules is reduced when a potential difference at the ionic double layer is present. Thus, the adsorption capacity of an electrode is, at its maximum, close to the potential of zero charge. In 1963, Antropove proposed a special scale of the potential, the initial value of which is the potential of zero charge of the surface  $E_{zch}$ . Then, the potential on this scale will be the difference between the steady-state potential of the electrode and the potential of zero charge.

For  $\Phi > 0$ , the metal will be positively charged relative to the electrolyte and a layer consisting primarily of anions will be adjacent to the metal surface on the side of the solution. For  $\Phi < 0$ , the metal will be negatively charged relative to the electrolyte and a layer consisting primarily of cations will be adjacent to the metal surface on the side of the solution. Knowledge of the potentials of zero charge of metals and the steady-state potentials in a given medium can facilitate considerably the search for a suitable corrosion inhibitor.

The value of  $E_{corr}$  obtained in the present study for HCl solution is  $-500$  mV versus SCE. When PVP was dissolved in a hydrochloric acid solution, protonation of the  $NH_2$  may occur. Benerijee and Mahotra [14] reported the pzc of iron equals  $-530$  mV versus SCE in hydrochloric acid solution. Therefore, the value of  $\phi$  is  $+30$  mV, so the metal surface acquires a positive charge.

For PVP, the nitrogen atom is protonated in acidic medium and adsorption of cationic  $-N^+$  on the C-steel surface does not take place. We propose that the  $-N^+$  group would be protonated to :



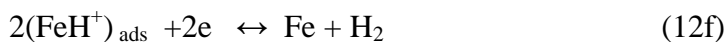
The presence of oxygen atoms in the PVP structure makes this protonation easier. Thus the  $Cl^-_{(aq)}$  ions will be associated with the  $-N^+$  atom in PVP molecules instead of attacking the C-steel

surface. The negatively charged oxygen with its lone pairs are attached to C-steel atoms with a coordinate bond that seems strong enough even at higher temperature, as shown in Table 4. Now we have a competitive reaction between the positively charged C-steel surface, the negatively charged oxygen, and the negatively charge  $\text{Cl}^-$ . The present results of the % IE of PVP even at 60 °C (Tables 3 and 4) indicate that PVP is strongly adsorbed on the C-steel surface (chemisorption). The PVP consisting of several units each has the structure indicated in Fig 1; thus, more PVP units are protonated in the presence of C-steel. Nevertheless, the helix structure of this polymer allows other units to be attached to the C-steel surface.

In HCl solution, the following mechanism is proposed for the corrosion of iron and steel [16]. According to this mechanism, the anodic dissolution of iron is:



The cathodic hydrogen evolution:



Taking into consideration all these references, the  $\Delta G^{\circ}_{\text{ads}}$  value and the  $E_{\text{app}}$  value calculated from the Arrhenius plots, the action of PVP as a corrosion inhibitor for C-steel in HCl may be attributed to a strong adsorption bond which is of a chemisorptive nature, involving charge sharing or charge transfer from the oxygen double bond in the PVP molecule to the positively charged C-steel surface to form a coordinate-type bond and an electrostatic attraction between the cationic  $-\text{N}^+$  species and  $\text{Cl}^-$ . Iron is a transition metal with vacant, low-energy electron orbitals and the loosely bound electrons of oxygen in the PVP molecule support this proposition for the adsorption mechanism. The hydrophobic part of PVP polymer is believed to face the solution with the added advantage of locking the chains strongly on the metallic surface.

The corrosion rates of 2 M HCl in the absence and presence of 4000 ppm of PVP was studied over a period of 168 hours. The % IE and the change of  $\Delta W/A$  with time for 2 M HCl solutions in the presence and absence of 4000 ppm of PVP are shown in Figure 8 and Figure 9. It was found that the maximum % IE was 75%, obtained after four hours of immersion, then it subsequently decreased. Following  $\Delta W/A$  with time for 2 M HCl solutions in the presence and absence of 4000 ppm of PVP showed a gradual increase until it reached a constant value after 72 hours of immersion for both solutions.

The inhibition efficiency results obtained from the electrochemical methods are in good agreement with each other but slightly higher than those obtained from the weight loss method, as shown in Figure 7. These findings are in agreement with reports in other studies [2, 8, 9]. This difference may be attributed to the fact that weight loss gives the average corrosion rates over the immersion time, whereas the electrochemical method provides the instantaneous corrosion rates.

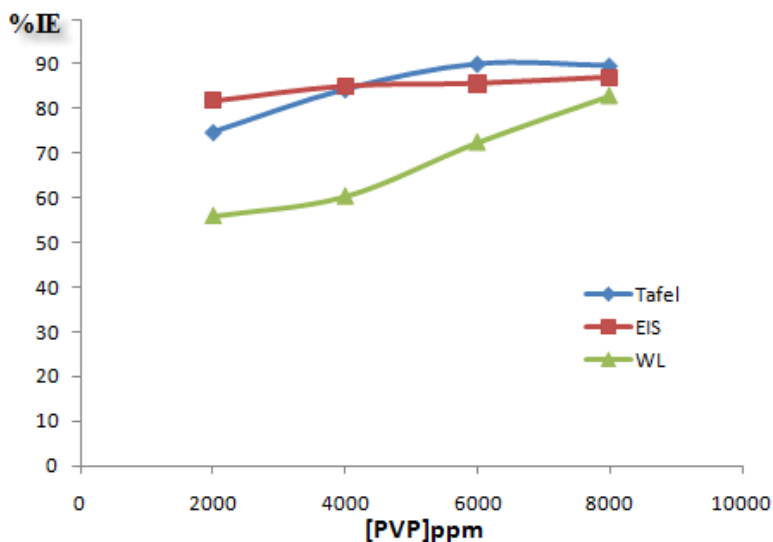


Figure 7. A comparison of % IE of the three methods: EIS, Tafel and WL.

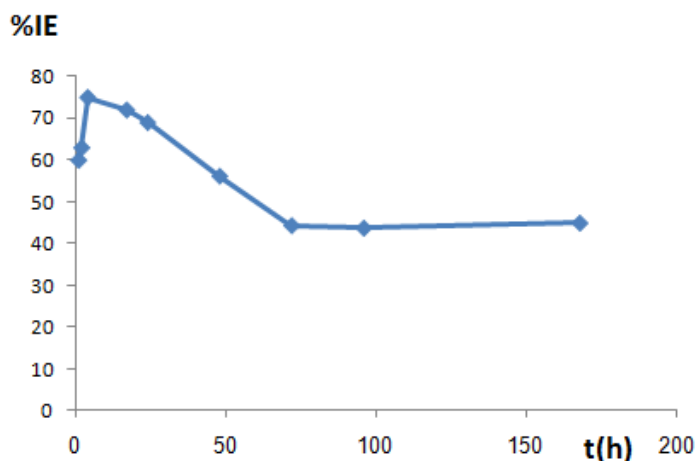


Figure 8. The change of inhibition efficiency with time for 2 M HCl solution in the presence of 4000 ppm of PVP at 30 °C.

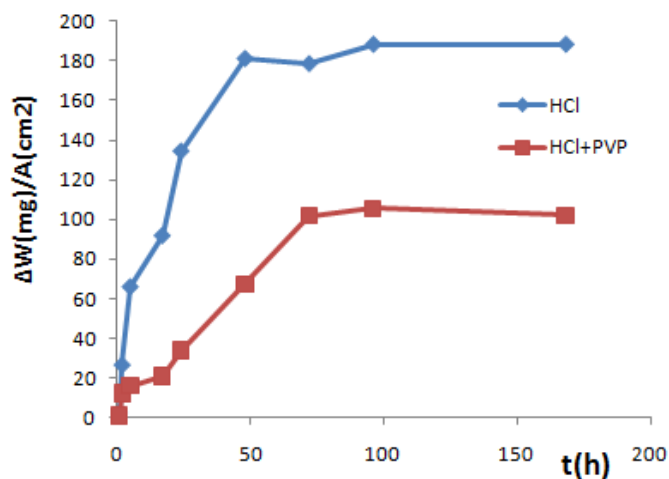


Figure 9. The change of ΔW/A with time for a 2 M HCl solution in the presence and absence of 4000 ppm of PVP at 30 °C.

#### 4. CONCLUSION

1. From the present study, it was concluded that PVP is a good corrosion inhibitor even at high temperatures. The maximum % IE was obtained after 4 hours of immersion.
2. From EIS results, it was found that the adsorption of PVP led to the formation of a protective film on the metal/solution interface and the increase in thickness of the electronic double layer.
3. From Tafel results, it is shown that PVP is a mixed-type inhibitor affecting the iron dissolution and hydrogen evolution.
4. From weight loss results, the Langmuir adsorption isotherm was obeyed. The inhibition efficiency of PVP increases with increasing inhibitor concentration and increasing temperature. The inhibitor showed the maximum % IE at 8000 ppm of inhibitor concentration for WL. For the EIS and Tafel, the % IE reached its maximum and remained almost constant at 4000–8000 ppm of inhibitor concentration.
5. From the change of pH values for HCl + PVP and HCl + PVP + C-steel solutions, the  $\Delta G^{\circ}_{\text{ads}}$ ,  $E_{\text{app}}$  values, and the positive nature of the C-steel surface in the present study, we may assume that the PVP molecules are chemically adsorbed through the negatively polarized oxygen atom.
6. The thermodynamic parameters support the % IE results of EIS, Tafel and WL, which show that PVP is a good corrosion inhibitor for C-steel in HCl solutions.

#### ACKNOWLEDGEMENTS

This research project was supported by a grant from the “Research Center of the Female Scientific and Medical Colleges”, Deanship of Scientific Research, King Saud University. The author is grateful for Al Jawharah Al Jahany and Hanan Al Magamsey for performing the WL experiments.

#### References

1. Y. Jianguo, W. Lin, V. Otteno-Alegoi and D.P. Schweinsberg, *Corros. Sci.*, 37 (1995) 975.
2. F. S. de Souza and A. Spinelli, *Corros. Sci.*, 51 (2009) 642.
3. L. Afia, R. Salghi, O. Benali, S. Jodeh, I. Warad, E. Ebenso and B. Hammouti, *Portugaliae Electrochim. Acta*, 33, No.3 (2015)137.
4. L. A. Al Juhaiman, A. A. Mustafa and W. K. Mekhamer, *Anti-Corros. Method M*, No. 1 (2013) 28.
5. B. A. Abd El-Nabey, E. Khamis, G. E. Thompson and J. L. Dawson, *Surf. & Coat. Tech.*, 28, No. 1 (1986) 83.
6. S. A. M. Refaey, F. Taha and A. M. Abd El-Malak, *Appl. Surf. Sci.*, 236 (2004)175.
7. A. Popova, E. Sokolova, S. Raicheva and M. Christov, *Corros. Sci.*, 45 (2003) 33.
8. A. S. Fouda, A. A. Al-Sarawy and E. E. El-Khatori, *Desalin.*, 201 (2006) 1.
9. S. V. Ramesh and A. V. Adhikari, *Mater. Chem. Phys.*, 115 (2009) 618.
10. S. M. A. Hosseini, M. Salari, E. Jamalizadeh, S. Khezripoor and M. Seifi, *Mater. Chem. Phys.*, 119 (2010) 100.
11. T. Szauer and A. Brandt, *Electrochim. Acta*, 26 (1981)1253.
12. A. Yurt, B. Balaban, S. U. Kandemir, G. Bereket and B. Erk, *Mater. Chem. Phys.*, 85 (2004) 420.

13. A. A. Hermas, M. S. Morad and M. H. Wahdan, *J. Appl. Electrochem.*, 34 (2004) 95.
14. G. Benerijee and S. N. Mahotra, *Corrosion (NACE)*, 48 (1992) 10.
15. K. S. Shukla and M. A. Quraishi, *Corros. Sci.*, 51 (2009) 1007.
16. Ashish Kumar Singh, Aditya Kumar Singh and Eno E. Ebenso, *Int. J. Electrochem. Sci.*, 9 (2014) 352.
17. L. A. Al Juhaiman, A. A. Mustafa and W. K. Mekhamer, *Int. J. Electrochem. Sci.*, 7 (2012)8578
18. J. R. Macdonald and D. R. Franceschetti, in: J. R. Macdonald (Ed.), *Impedance Spectroscopy*, Wiley, New York, 1987.
19. H. Ashassi-Sorkhabi, N. Ghalebsaz-Jeddi, F. Hashemzadeh and H. Jahani, *Electrochim. Acta*, 51 (2006) 3848.
20. K. Aramaki, M. Hagiwara and H. Nishihara, *Corros. Sci.*, 5 (1987) 487.
21. A. S. Fouda, H. A. Mostafa, F. El-Taiband G. Y. Elewady, *Corros. Sci.*, 47 (2005) 1988.
22. M. A. Quraishi and S. K. Shukla, *Mater. Chem. Phys.*, 85 (2004) 420.
23. H. H. Uhlig, *Corrosion and Corrosion Control*, 2nd Ed., John Wiley and sons Inc. 1971.
24. K. Shalabi, Y.M. Abdallah, Hala M. Hassan and A.S. Fouda, *Int. J. Electrochem. Sci.*, 9 (2014) 1468 .
25. R. Solmaz, G.Kardas, M.Culha, B.Yazici and M.Erbil, *Electrochim. Acta*, 53 (2008) 5941.
26. B. Zerga, B. Hammouti, M. Ebn Touhami, R. Tourir, M. Taleb, M. Sfaira, M. Bennajeh and I. Forssal, *Int. J. Electrochem. Sci.*,7 (2012) 471.

© 2016 The Authors. Published by ESG ([www.electrochemsci.org](http://www.electrochemsci.org)). This article is an open access article distributed under the terms and conditions of the Creative Commons Attribution license (<http://creativecommons.org/licenses/by/4.0/>).